RESEARCH ARTICLE

Analysis and mitigation of nonuniform soiling distribution on utility-scale photovoltaic systems

Leonardo Micheli | Eduardo F. Fernández | Álvaro Fernández-Solas |
João Gabriel Bessa | Florencia Almonacid

Advances in Photovoltaic Technology
(AdPVTech), CEACTEMA, University of Jaén
(UJA), Jaén, Spain

Correspondence
Leonardo Micheli, Advances in Photovoltaic
Technology (AdPVTech), CEACTEMA,
University of Jaén (UJA), Las Lagunillas
Campus, Jaén 23071, Spain.
Email: lmicheli@ujaen.es

Abstract

The present paper evaluates the soiling losses of a 3.25-MW photovoltaic (PV) system installed in central Chile, 200 km north of Santiago, and analyzes the nonuniform soiling deposition between the various strings for a period of 3 years. A robust methodology is developed to extract, in the most systematic way, 142 reliable soiling profiles from the 256 PV power time series recorded on site. It is found that, if unmitigated, soiling would reduce the annual DC energy generation by 8%, with a factor of $2\times$ between the losses of the most and least affected strings. Most of the losses are registered on the edges of the plant, closer to traffic and unpaved roads. The most soiling intense months are in summer, result of the infrequent rainfalls and of the high concentrations of suspended particles that characterize this season. The revenues and the costs of different manual cleaning frequencies are evaluated and compared to identify the optimal soiling mitigation strategy for this site. Three cleanings per year are found to return the highest profits for the economic conditions considered in this study. However, a sensitivity analysis shows how different cleaning costs and electricity prices would affect the soiling mitigation strategy. In addition, in light of the nonuniform soiling deposition distribution, the possibility of cleaning only selected strings rather than the full PV plant is discussed.

KEYWORDS

Chile, cleaning optimization, mitigation profits, photovoltaic performance, soiling

1 | INTRODUCTION

Soiling consists of the accumulation of dust and dirt on the surface of photovoltaic (PV) modules and causes significant energy and economic losses to PV systems worldwide. A recent investigation found soiling responsible for average energy yield losses in between 4% and 5% and for yearly missed revenues of at least €3 billion globally.[1] Because of this tangible impact and driven by the increasing deployment of new PV capacity in high insolation and high soiling regions, the number of publications on soiling has risen exponentially in the last decade.[2,3] Differently from other PV reliability issues, soiling is generally reversible and can be mitigated through an adequate and site-specific cleaning schedule. In this light, several models have been proposed in literature to optimize the operating and maintenance (O&M) actions, minimizing the soiling losses and, at the same time, limiting the mitigation costs.[4-7] However, these studies on soiling economics and cleaning optimization have not taken into account that soiling can deposit at different rates over large PV systems.[8]

System-level soiling nonuniformity is a known but still relatively unexplored issue, which causes an uneven distribution of soiling between the various strings of the same site.[8–11] In order to identify nonuniform soiling, the IEC 61724-1 standard recommends more than one soiling measurement for sites ≥5 MW expecting soiling losses ≥2%.[12] Factors >2× were found between the soiling deposition rates of modules of the same PV sites in California.[9] Losses varying between 5% and 11% were shown for another Californian site.[11] In order to improve the understanding of soiling deposition over large PV systems, a study[10] investigated and mapped the wind patterns for different rows of PV modules of a PV facility in Nevada, taking also into account the effect of the wind direction. Despite all these findings, the possibility of cleaning only selected strings of a PV system depending on the soiling distribution has not been yet addressed in literature.[1]

The present work analyzes the performance and the soiling losses of a utility-scale 3.25-MW PV system in Chile. The effects of non-uniform soiling distribution across the various strings of the PV systems, an issue expected to increasingly affect plants worldwide given also the growing share of utility-scale PV systems,[13] are specifically investigated. This is made possible through the analysis of the soiling profiles of the 256 pairs of strings of the system, which are independently and systematically studied. This represents the largest pool of data on soiling measured within the same PV site. The results of this analysis are used to assess revenues and profits of different cleaning strategies and to evaluate the profits of cleaning each individual string. The possibility of cleaning only highly soiled strings rather than the full PV plant to improve the soiling mitigation profits is also evaluated. In addition, the paper provides novel information on the PV performance in Chile, a country with a high solar potential and where significant investments are being made but that is exposed, at the same time, to severe soiling risks.

The paper is structured as follows. A brief overview on the status of PV and on the literature available on soiling in Chile is given in Section 2. Section 3 presents the characteristics of the site where the system is installed (Section 3.1) and the methodologies employed to analyze the PV performance data (Section 3.2), to extract and model the soiling loss profiles (Sections 3.3 and 3.4), and to evaluate the profitability of various cleaning frequency scenarios (Section 3.5). The analysis of the soiling losses is presented in Section 4. Last, the results of the cleaning optimization are discussed in Section 5. Additional figures are available in the Supporting Information to back the decisions made in the soiling extraction process and to help understanding some of the results. These are referenced in the text as "Figure S."

## 2 | PV PERFORMANCE AND SOILING IN CHILE

The plant focus of the present study is located in Chile, one of the countries experiencing the most intense PV capacity growth worldwide. Since 2012, the national PV capacity has gone from 3 MW to >3 GW in September 2020,[14,15] with more than 450 MW installed every year since 2014. PV already produces more than 8% of total electricity generation in the country.[16] This PV expansion is being pushed by the high solar resource and the favorable market conditions[17,18] that have led to levelized costs of electricity among the lowest worldwide.[19] However, the performance and the revenues of PV systems in Chile can be severely affected by soiling. Annual soiling losses were found to significantly vary within the country, with peaks as high as 39% in the northern coastal area of the Atacama Desert.[20] If not opportunely mitigated, soiling can substantially affect the PV performance, lowering the profits and limiting the deployment of new PV capacity.

Because of these conditions, soiling of Chilean PV systems has started receiving some attention in the past years, and a recent review has highlighted the need for additional studies on the impact of the environmental and soiling conditions on PV in Chile.[17] Several works on this topic have been conducted in the capital city, Santiago, and focused on the impact of soiling on different PV technologies.[5,21,22] In Santiago, the highest soiling deposition rates were found to take place in the winter months due to the higher particle concentrations occurring in this season.[5] However, higher soiling rates do not directly translate into higher soiling losses as these are also affected by rainfalls, which are more frequent in winter.[21] The same seasonal soiling deposition rate trends were also reported for Santiago in a different study,[20] which was conducted in five additional locations across the Atacama Desert. In that study, significant losses (>3%/year) were found only for the two northernmost and driest investigated sites, in addition to Santiago. A different investigation, also conducted in northern Chile, reported transmittance losses higher than 50% for PV glasses exposed for just 4 months.[23] Another work compared the performance and the soiling losses of two PV technologies in coastal northern Chile.[24] Power losses >9% were reported for a polycrystalline module installed in a different coastal area of the Atacama Desert after 4 month of exposure.[25]

All these investigations have provided essential information on the performance and the soiling of PV in a country as Chile. Despite that, most of them focused on Santiago or in the northern part of the country only. The PV system here investigated is at the center of a 400 km north–south transect, delimited approximately by the longitudes 29.9°S and 33.5°S, in which no soiling investigation was previously conducted, as shown in Figure 1 (more information on the characteristics of the location in Section 3.1). For this reason, the present study also provides useful data on the solar potential of a region with high insulation in a country currently experiencing substantial PV investments.

Some of the previous works also presented cleaning optimization models.[5,20,22] These are of value and provide important information on the profits and costs of PV soiling mitigation in Chile. However, they are all based on data collected from soiling measurement devices or few-kW-scale PV systems. Therefore, they do not take into account the potential nonuniform soiling distribution that can affect larger PV systems and that is the main topic of the present work.
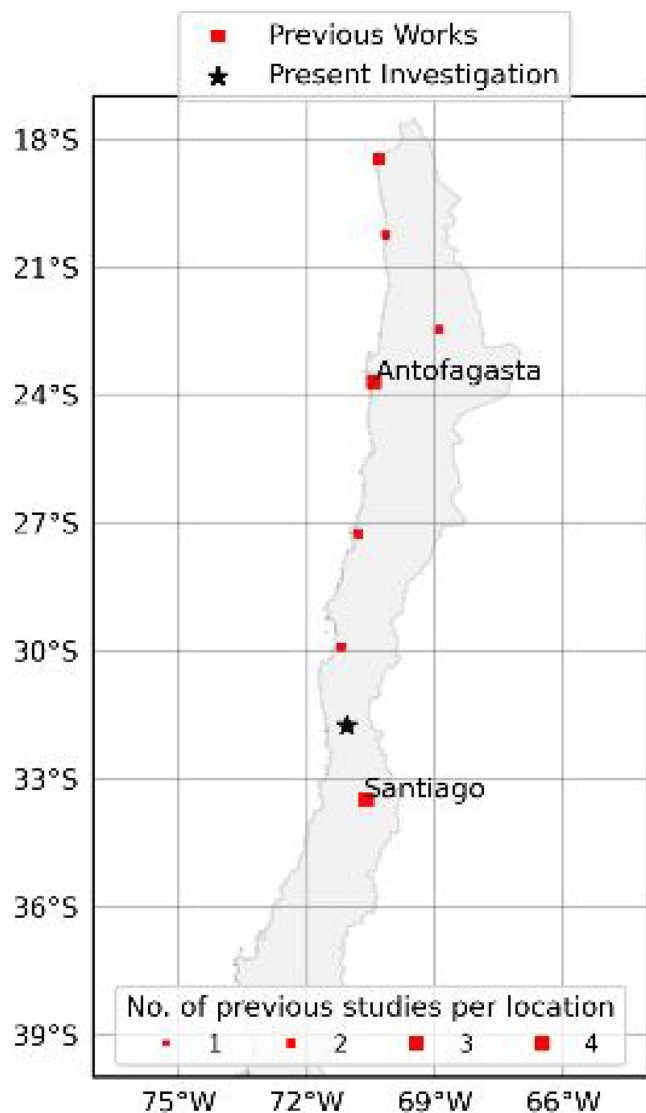
FIGURE 1 Map of Northern Chile with locations of the previous studies on PV soiling.[5,20-24] The previous works' markers are sized depending on the number of studies conducted in each location. The locations of two sites in Olivares et al.,[23] labeled as "Northern Desert," could not be identified and have not been included

3 | MATERIALS AND METHODS

3.1 | Location

The data of this study are sourced from a 3.25-MW PV system located in the Coquimbo Region, Central Chile, about 200 km north of Santiago and 40 km west of the closest seashore, at 365 m of altitude. The site is at the border between BSk (cold arid steppe) and Csb (warm temperate summer dry) climate zones according to the Köppen–Geiger classification.[26] On average, this location receives a radiation of 2400 kWh/m^2/year at optimal tilt, 6% more than Santiago and higher also than that of the northernmost coast of the Atacama Desert.[27] As shown in the top plot of Figure 2, the region is

characterized by frequent and intense precipitations in winter (June to September) and longer dry spells in summer (October to March). Over the last 30 years, it has experienced on average 261 mm of rainfall per year, more than 70% of which typically in between May and August (data sourced from MERRA-2,[28] events <1 mm/day are excluded). On average, dry spells last less than 20 days in winter (April to September), while they can be as long as 44 to 46 days in October and November. The middle plot in Figure 2 shows the typical daily wind speeds (left y axis), calculated as simple average of the daily means in between 1980 and 2019, and the daily maximum wind speed distribution (right y axis) over the same period. As it can be seen, the average wind speeds are in between 2.5 and 3.5 m/s from October to March and below this range during the remaining months of the year. On the other hand, April to September is the period in which the highest and most frequent wind gusts are registered.

3.2 | PV performance

The PV system consists of 508 strings of 320 W-rated polycrystalline modules mounted facing north at 20° tilt. The analysis is conducted on the hourly DC power data measured at the combiner boxes from January 2017 to December 2019. Two hundred fifty-six time series were provided, 252 of which reported the combined electrical output of two strings (40 modules and 12.8 kW per time series) and four of which reported the output of an individual string of 20 modules.

Global tilted irradiance and ambient temperature are also measured at the site through a pyranometer and a NTC thermistor, respectively. The same measurements, taken on the east side of the plant, are used for all the string pairs. The sensors are maintained regularly and cleaned every week by the O&M team. This is the minimum cleaning frequency recommended by the IEC 61724-1 standard[29] to maintain the highest irradiance measurement accuracy. It is acknowledged that, within the week, soiling of the irradiance sensors might occur in some cases. However, unfortunately, no method has been proposed yet to evaluate the soiling of irradiance sensors and to correct accordingly the measurement profile. So no action could be taken in this regard, but future works should address this issue. However, even if the soiling deposition on the irradiance sensors is present, it is not expected to affect substantially the detection of the nonuniform soiling distribution, which is the main focus of this work.

The hourly wind speed and rainfall intensity data have been instead sourced from MERRA-2[28] through the soda-pro web interface.[30] MERRA-2 data are originally available at a 0.625° × 0.5° spatial resolution. So the four closest MERRA-2 data points were processed through bilinear interpolation to generate the time series from the investigated site.

The performance ratio of each string pair has been calculated as the ratio of the measured to the expected power outputs. The latter has been estimated from the irradiance by applying temperature, spectral, and angular corrections available in *pvlib-python*.[31] The temperature correction was based on the methodology proposed by King
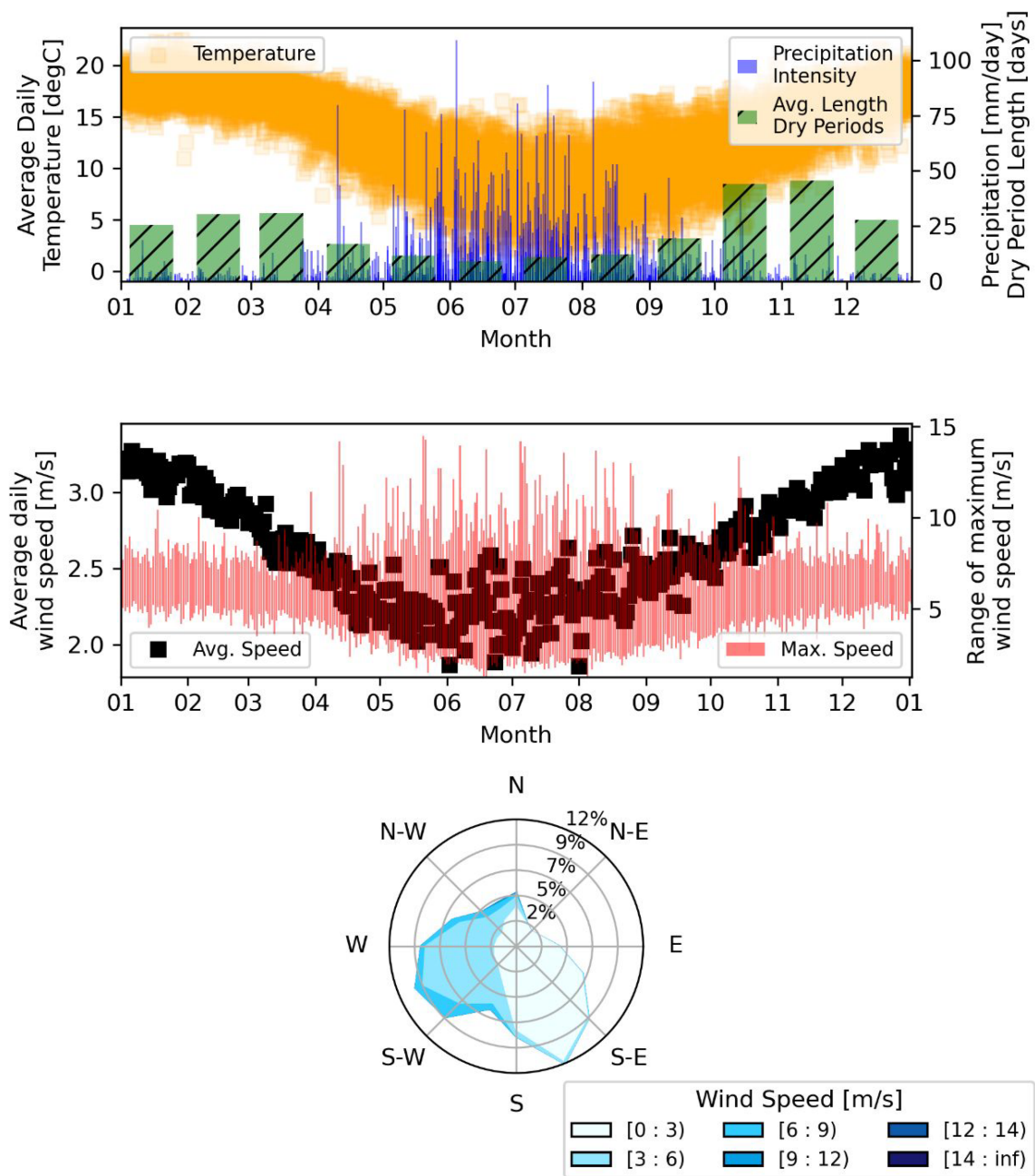
FIGURE 2 Weather characteristics from 1980 to 2019 at the location of the study. Top plot: daily ambient temperatures in °C (orange squared markers, left y axis), daily precipitation intensities (blue bars, right y axis) in mm/day, and monthly average length of the dry spells (hatched green bars, right y axis) in number of days. Middle plot: average daily wind speeds (black squared markers, left y axis) in m/s and distribution of the maximum daily wind speeds (red vertical bars, right y axis) also in m/s. Bottom plot: wind rose showing the frequency of winds blowing from each direction. Original hourly data sourced from MERRA-2 database,[28] through the soda-pro.org platform. Only precipitations of intensity >1 mm/day have been considered. Wind speeds and directions refer to winds at 10 m above ground

et al.[32] The ASHRAE model was employed to estimate the incident angle modifier.[33,34] The spectral losses were calculated from the air mass using referenced methodologies.[35,36] All the parameters needed for the corrections were set as those of a polycrystalline 72-cell glass-cell-polymer module on the Sandia module database.

No inverter clipping has been detected. Data from October 6 to November 15, 2017, have been discarded because of a shading issue due to the development of the undergrowth (removed on November 14) affecting some of the strings. Outlier filters similar to those employed by Theristis et al.[37] were also applied: only hours with irradiance between 50 and 1300 W/m^2 and performance ratio between 0.1 and 1.3 were considered. In addition, any hourly data point outside the two standard deviations, calculated from the whole time series, was removed.[37]

3.3 | Soiling extraction

Soiling has been quantified through the soiling ratio, a metric that expresses the ratio of the electrical output of a PV device to the electrical output that the same device would have in clean conditions.[12] In this work, the soiling ratio calculation was based on the DC power data. Soiling losses were calculated as 1 − soiling ratio and expressed in %. A soiling ratio of 1 corresponds to 0% losses, and its value lowers (i.e., the losses raise) while soiling accumulates on the PV modules' surface.

A time series of daily soiling ratio values ("soiling profile") was extracted for each string pair from the PV performance ratios, previously calculated from the DC power data (Section 3.2). The methodology employed to extract the soiling profiles, partially based on previous works, was made of the following steps:

i. Daily performance values were calculated as the simple average of the hourly data within 1 h of the solar noon. Only data with global tilted irradiance >700 W/m^2 were kept.[38] These conditions are stricter than those recommended by the IEC 61724-1 standard[12] or employed in previous works[39–41] but (i) take into account the fact that the analysis is conducted in a high irradiance region and (ii) are expected to minimize the noise in soiling extraction.

ii. Any daily value on a day i outside of two standard deviations of the mean of the values calculated from the data within $i − 7$ and $i + 7$ was considered an outlier.[42]

iii. Any missing daily data point was filled using the Next Observation Carried Backward method. The 14-day window rolling median was calculated from the performance ratio and normalized to the 95th percentile value.[43]

iv. The effect of degradation was removed from the normalized performance ratio profile. Each daily performance ratio was divided by the degradation rate value, extracted through the year-on-year decomposition function available on *rdtools*.[44,45]

v. The impact of artificial cleanings on the PV performance was removed, and any natural cleaning was identified through the analysis of positive shifts in the soiling ratio profiles.[43] The methodologies employed in this step are detailed in Section 3.4.

vi. Each period of at least 14 days within two natural cleanings was fitted through a piecewise regression.[42,46] If the change point was found to occur within 7 days of one of the natural cleanings, linear regression was employed instead. A flat profile was modeled for deposition periods shorter than 14 days or with fits of R^2 < 0.7. The minimum number of days was set in agreement with Deceglie et al.[47] to avoid fitting extremely short periods, which could have led to unrealistic soiling rates. The R^2 threshold, based on Kimber et al.,[48] helped to prevent the extraction of soiling rates from extremely noise or poorly fit data.

vii. The soiling profile was adjusted so that cleanings restored the value of the daily soiling ratio to 1.0.[5] Each data point of a soiling period in between cleanings was therefore moved to set the first daily value at 1.0.

Performance ratio profiles missing more than 30% of the soiling data points (i.e., days) in total or missing more than 5% of data points (i.e., days) consecutively were discarded. In addition, from the visual inspection of all the time series, it was also found that an R^2 of 0.83 and a mean absolute error (MAE) of 0.03 could successfully identify acceptable soiling profiles when these were compared to the performance ratio profiles. The valid soiling profiles with the highest and the lowest R^2 are shown in Figure S1 ("S" denotes that the figure is reported in the Supporting Information). Figure S2 shows the valid soiling profiles with the minimum and maximum MAEs. Examples of the discarded soiling profiles are shown in Figure S3.

The filtering procedure left 142 valid string pairs out of the initial 256. Therefore, the sample here investigated represented the 55% of the total PV site capacity. The profiles of the most and least soiled valid string pairs are shown in Figure 3. It is acknowledged that the filtering is stricter and the developed model is more complex than those presented before.[43,48] This is motivated by the fact that the data used in this work represent the largest data pool used so far on a single soiling study. This large number of inputs made untrustworthy to manually or visually tune each time series independently (as done previously) and led to the necessity of developing a model to analyze the data in the most systematic and robust way, at cost of neglecting a number of time series. A map of the average normalized performance of the various strings of the plant is shown in Figure S4.

It should be noted that some authors have used an exponential function to model soiling accumulation[7] or assumed that the soiling accumulation would slow down or stop after a certain threshold.[6] However, the present work makes use of linear soiling trends; soiling is assumed to accumulate at fixed rates in between cleanings. This approach is the same used in several previous works[5,38,43,48] and was chosen because of its simplicity (it did not require to set an arbitrary soiling accumulation limit or threshold) and because widely accepted and used in the literature.

3.4 | Cleanings: Removal, identification, and modeling

In this section, the methodologies related to the modeling of natural and artificial cleanings are described. First, the method employed to remove the effect of artificial cleanings from the soiling profile is described. Second, the procedure adopted to identify natural cleaning events is detailed. Last, the methodology used to investigate the effects of different cleaning schedules on the soiling loss profile is reported.

Nine artificial cleaning events were performed by the O&M team in between January 2017 and December 2019 on dates that were provided to the authors. It should be noticed that there is no accepted methodology in the literature to remove the effects of artificial cleanings from a soiling profile. So a procedure similar to that employed for different sites in previous works[20,38,49] was established and employed. The methodology is based on the procedure commonly used to model the effect of cleanings on an unmitigated soiling
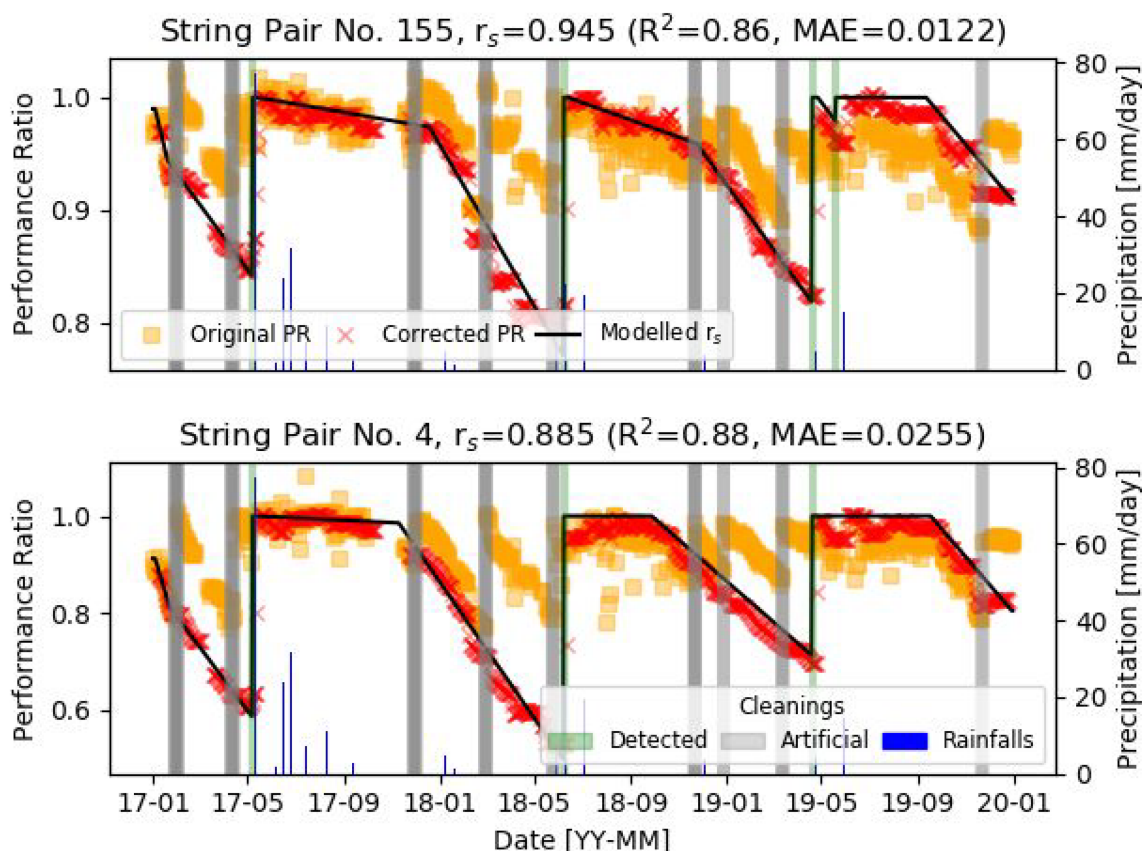
FIGURE 3 Valid extracted soiling profiles with the highest and the lowest average soiling ratio value (r_s). Orange square markers: original normalized performance ratios extracted from power data. Red cross markers: daily performance ratios after normalization and removal of artificial cleanings (points iv and v of the procedure described in Section 3.3). Black line: extracted soiling ratio profile. Green vertical bars: detected cleaning dates.[43] Gray vertical bars: artificial cleaning dates. Blue bars: rainfall events in mm/day reported[28] by MERRA-2

profile.[5,50] Indeed, cleanings are typically modeled to generate a positive shift on the soiling ratio that propagates until the following cleaning date. So, in this case, all the data points following an artificial cleaning and until the following natural cleaning were lowered by a value equal to an offset, calculated as the difference in the average soiling ratio between the first week after and the last week before the cleaning was performed. The artificial cleaning was modeled not to affect the magnitude of the daily variation between of consecutive data points (i.e., the soiling rate). The methodology employed to identify the natural cleaning events is detailed in the following paragraphs.

Soiling extraction is typically performed by fitting data points in between natural cleaning events. These can be identified through one of two methodologies. The most common approach is based on the assumption that any rainfall event above a certain threshold has a cleaning effect on soiling. This method requires in input the rainfall pattern and a minimum cleaning threshold value. Several thresholds have been used or reported in literature, ranging from 1 mm/day[40,51] to values ≥5 mm/day.[4,52] In addition, a study also reported that rainfalls of similar intensities had cleaning effect on one season but did not affect soiling in another season.[53] Something similar happens for the given site: a 4.6-mm/day rainfall event on January 8, 2018, and a

3.8-mm/day rainfall event on December 4, 2018, did not have any effect on soiling, whereas a 4.5-mm/day event on April 23, 2019, completely washed off the dust from the modules. Therefore, the possibility of using rainfalls for cleaning identification in this work was discarded. This decision made it possible to investigate the cause of the natural cleanings, rather than assuming a priori rainfalls as dominant cleaning agent.

The second common cleaning identification approach does not require in input the rainfall pattern and detects the cleanings directly from the positive shifts of the soiling ratio profile.[43] Any positive shift larger than a set threshold is identified as a cleaning. In the original formulation proposed by Deceglie et al.,[43] the threshold is set as $P_{75} - 1.5 \cdot (P_{75} - P_{25})$, where P_{75} and P_{25} are the 75th and 25th percentiles of the absolute values of daily variations in performance ratio. However, due to the noise in some of the soiling profiles, this algorithm can occasionally label outliers as "cleaning events," even if no natural cleaning occurred. These events (here called "false cleaning") can be visually determined because the positive shift (i.e., the cleaning effect) affects only one or at most a limited number of noisy data points, after which the soiling profile returns to the previous level. It is worth emphasizing that the cleaning identification process is

conducted independently of the weather pattern and that the "false cleanings" are not associated to a particular cleaning agent (e.g., a cleaning is not label as "false" because caused by wind) but are rather the effects of the noise in the data. The data gathered from PV plants' performance are indeed subject to more noise than soiling stations, which have been typically used in soiling studies. An example can be seen in the left plot of Figure S5, where a "false cleaning" is detected by the algorithm in the fall of 2018. However, the trend of the data points after that detected cleaning suggests that the cleaning did not actually occur, as, after it, the soiling ratio continues decreasing from the same value as before. A visual analysis proved that "false cleanings" were detected in many time series and that the detection algorithm worked with different accuracies on different pairs of strings, making their comparison unreliable. A similar issue was reported previously,[54] and it was addressed through a time series specific tuning of the threshold equation. However, due to the number of time series investigated in this work, the time series specific calibration was discarded, because it would have required a different arbitrary choice for each time series, as no fixed threshold was found to be accurate for all the time series.

The first and most significant improvement in cleaning detection was found by removing short periods of high noise (February 24 to March 11, 2017; May 7–19, 2017; April 8–11, 2018; April 21–25, 2019; November 2–10, 2019; and November 22–27, 2019) from all the performance ratio profiles. In addition, it was decided to ignore any cleaning identified through the original threshold equation[43] that did not cause a positive shift in the soiling ratio larger than 0.03 (Figure S5). This approach required to perform the soiling extraction twice, once to remove the false cleanings and once to generate the final soiling profile. Indeed, false cleaning identification had to be conducted on the extracted soiling ratio profile to avoid the threshold to be biased by noise and outliers, which can be particularly frequent and severe in rainy days. This approach is therefore less computationally efficient than the methods proposed before, but it was necessary for a robust, reliable, and systematic analysis of the multiple time series. In addition, it should be noted that this approach discarded some of the cleanings in winter that had smaller effect on the soiling profile. This was found to have only a limited effect on the soiling extraction, also thanks to the adoption of a piecewise regression. Indeed, piecewise regression makes it possible to distinguish the high and the low soiling periods without the need for detecting intermediate smaller cleanings or changes in environmental conditions.[42] In addition, the 0.03 threshold was found to be particularly useful for those time series in which false cleaning events were still detected in the middle of the most soiling intense season. This approach is not expected to be immediately valid for other studies but can provide a baseline toward the development of more accurate, universally valid, and self-calibrating methods for PV cleaning identification that should be investigated in the future.

The O&M cleaning schedule optimization was conducted by modeling various cleaning frequency scenarios and by comparing their effectiveness, their costs, and the additional revenues they generated. The optimal cleaning dates for each cleaning frequency scenario (i.e., cleaning dates that minimize the energy soiling loss given a number of cleanings, n_c) were estimated using the model described in previous works.[38,49] The same cleaning dates were modeled in each of the 3 years of data. Each modeled cleaning was assumed to restore the soiling ratio to 1, and a fixed offset was applied to all the following dates until the subsequent cleaning. The cleanings were modeled not to affect the soiling rates but only to have an effect on the soiling ratio. The costs and benefits of each cleaning were estimated through the methodology described in the next section.

3.5 | Economics and cleaning optimization

The most profitable cleaning frequency was selected by identifying the number of cleanings that maximized the soiling mitigation profits. These were calculated as the difference between the revenues (R) due to the recovered energy and the cleaning costs (CC), as described by Besson et al.[5] The soiling mitigation revenues (R), over the investigated period, were calculated as

$$R(n_c) = p \cdot 0.95 \cdot \sum_{s=1}^{S} \sum_{i=1}^{I} E_{s,i} \cdot (r_{s,i,nc} - r_{s,i,0}), \qquad (1)$$

where p is the electricity price ($0.16/kWh in Chile, as in Besson et al.[5]) and $E_{s,i}$ and $r_{s,i,nc}$ are the daily soiling-free energy yield and the daily soiling ratio on the day i, for the sth string and for a n_c number of cleanings. $r_{s,i,0}$ is the daily soiling ratio if no mitigation is performed. S is the number of strings for which a valid soiling loss profile was extracted. I is the total number of days of data collection. Only DC power data were provided; so a fixed typical 0.95 inverter efficiency was considered to convert these into AC values. The soiling-free DC energy yield was obtained as

$$E_{s,i} = \frac{\sum_{h=0}^{24} W_{h,s}}{r_{s,i,a}}, \qquad (2)$$

where W_h are the DC hourly power data and $r_{s,i,a}$ is the "actual" daily soiling ratio on the day i, for the sth string, calculated taking into account (i.e., not removing the effects of) the nine artificial cleanings. Missing data in October and November 2017 were replaced with the data from the same period of 2018. An example of the extracted performance and energy data is shown in Figure S6.

The total cost for each soiling mitigation scenario with an n_c number of cleanings was calculated as

$$CC(n_c) = \sum_{s=1}^{S} n_c \cdot C_w \cdot n_y, \qquad (3)$$

where C_w is the specific cleaning cost, per unit of power, and n_y is the total number of years. C_w was set equal to the minimum value ($1.9/kW/cleaning) found by a survey conducted for rooftop PV systems of 100 kW in 2016.[55] For the PV modules installed at the investigated

site, this corresponded to ~$0.3/m²/cleaning. A sensitivity analysis on the effect of different C_w values and of different electricity prices on the results is presented in Section 5.3.

The optimization was conducted by modeling a number of cleanings equal to the investigated cleaning frequency on the soiling profile of each string pair. Cleanings were modeled to restore the soiling ratio to 1 and to have no effect on same soiling rate (i.e., the slope of the soiling ratio profile). This means that a positive offset was applied to all the days after the cleaning until the following cleaning event. The revenues of each profile were calculated as for equation (1) and compared with the costs of equation (3) to calculate the profits.

Six cleaning frequency scenarios were considered, with a yearly number of cleanings going from 0 to 5. Differently from previous studies,[5,20] cleanings were not modeled at fixed intervals. For each cleaning frequency scenario, the soiling profile of each string pair was modeled. At each iteration, the same cleaning dates were modeled for all the years. For each cleaning frequency, the combination of cleaning dates returning the highest profits was selected as the optimal cleaning schedule. Cleaning dates were modeled at a 14-day step.

4 | SOILING LOSSES

4.1 | Soiling distribution

All the valid soiling profiles generated in this analysis are plotted in Figure 4. The average soiling ratio is 0.919, and the standard deviation is 0.013. The distribution of average losses is lightly skewed left (skewness: −0.6): 48% if the string pair experiences losses in the range from 6.5% to 8.0%. About 8.5% of the string pairs show losses

>10%, up to a maximum value of 11.5%. There are a 6.0% difference and a factor of 2.1× between the losses of the string pairs experiencing the most and the least soiling (right plot of Figure 4).

The left plot in Figure 4 also shows that the strings have in most cases the same natural cleaning dates. It is worth noticing that the three main natural cleaning events occur at the end of each summer (May 2017, June 2018, and April 2019) in correspondence with a rainfall. Another rain-based cleaning event is found in May 2019 for >60% of the string pairs. Additional smaller cleanings, reported by at least five strings pairs, were detected in May 2017, May 2019, and September 2019. These results and the profiles plotted in Figure 4 suggest that the cause of the dissimilar soiling ratios among the string pairs is mainly due to the different deposition rates in summer. During the winter months, indeed, the soiling accumulation is limited in all the strings, even because probably soiling is periodically washed off by undetected natural cleaning events. On the other hand, during the summer months (December to February), the soiling rates of the various string pairs can vary more significantly, with factors of 2× to 3× in between the maximum and minimum rates.

By knowing the design of the PV plant, it is possible to retrieve and map the soiling distribution depending on the position of each string, estimating also the average soiling ratio of missing strings through spatial interpolation.[39] Figure 5 shows that most of the losses occur on the northernmost and southernmost strings. However, it is only possible to speculate on the causes of this loss distribution, as the lack of locally measured environmental parameters does not make it possible to provide more specific and definitive answers. All the strings located in the first six rows from the south show average soiling ratios <0.9. The satellite imagery of the site shows that these strings are the nearest to the main road and are located 30 to 50 m from an unpaved lay-by where heavy vehicles operate. Along with the
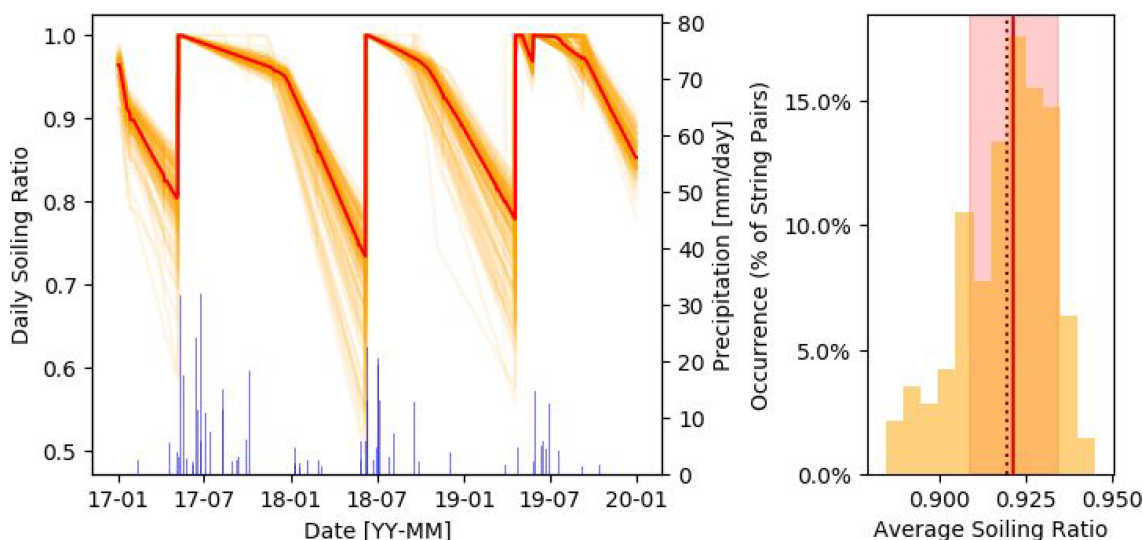
FIGURE 4 Left: soiling profiles of all the string pairs with valid soiling profile (orange lines). The red darker line shows the median soiling profile. Rainfalls are represented by vertical blue lines. Right: distribution of the average soiling ratios. The red vertical continuous line shows the median, the darker dotted line marks the mean, and the red area delimits the standard deviation. The time series with the highest and the lowest soiling losses are shown in Figure 3

closer position to the soiling sources, these strings are also possibly acting themselves, at least partially, as barriers to the transportation of dust over the central part of the PV plant.[57] However, unfortunately, this hypothesis cannot be confirmed at this time, given also
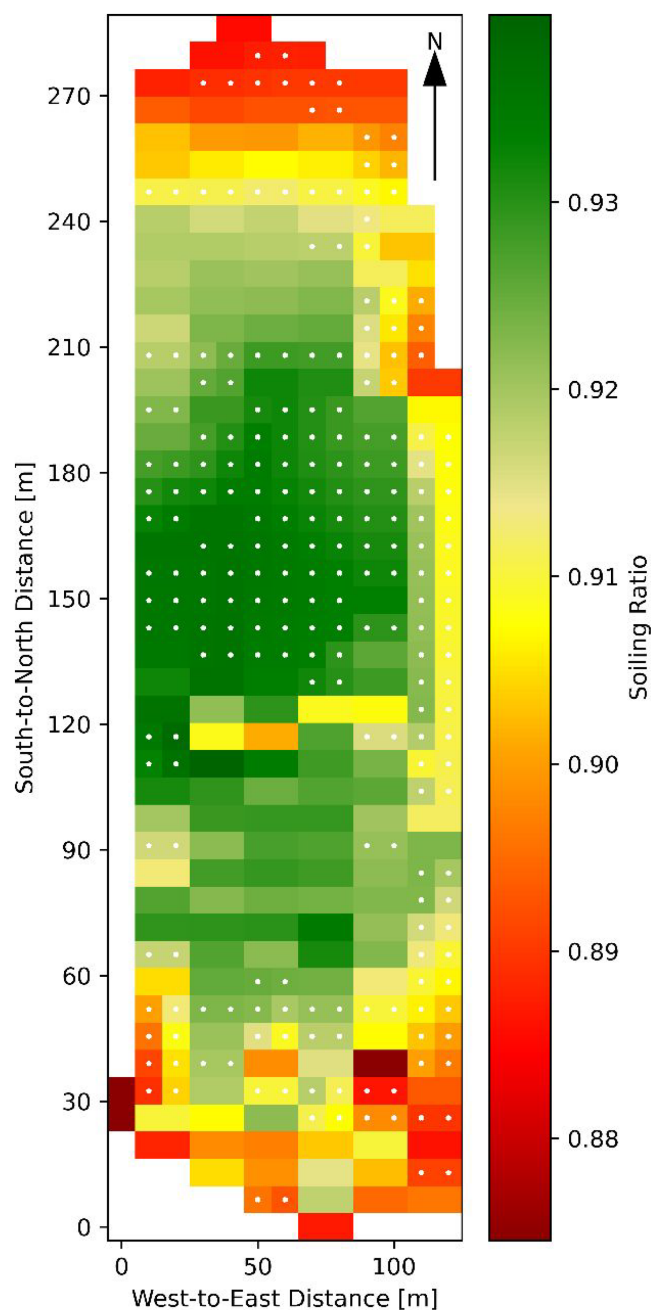
FIGURE 5 Geographical distribution of the strings and of the relative soiling losses. Each marker represents a string of 20 modules and is color coded depending on the severity of the soiling losses (dark green: 6.5%, dark red: 12.5%). Strings of the same pair have the same losses, so their markers have the same color. The soiling ratio of strings with nonvalid soiling profiles was estimated using linear spatial interpolation method available in the Python's SciPy package.[56] These strings are marked with a white dot. The same plot without spatial interpolation is shown in Figure S7

the fact that soiling of some strings had to be interpolated, and should be further investigated in future works. In addition, the entrance to the site and the service buildings are located on the north side, which potentially cause the cluster of high losses registered in that section of the PV plant. Last, the service road runs along the east side of the plant, connecting the main road and the entrance, and is potentially responsible for the soiling occurring on the easternmost strings. For these reasons, it is reasonable to think that in this particular case, the soling distribution could be due to the surrounding areas of the PV plants. However, the impact of other environmental parameters, such as wind speed and direction, should be considered in future works in order to achieve more solid result for both this and additional power plants.

4.2 | Soiling seasonality

From the analysis of the seasonality of the losses (Figure 6), it is possible to split each year into two consistently alternating periods: a high loss season in summer, peaking from February to April (median soiling ratio <0.87), and a limited loss period in winter (June to September, median soiling ratio >0.97). Soiling starts accumulating in August, at the end of the rainiest months (Figure 2), and the high loss season terminates with the first intense cleaning event, which generally takes place in between April and May.

As also previously shown in Figure 4, one of the causes for the seasonal soiling is the yearly pattern of rain. Rain events are frequent in winter (April to September), keeping the PV modules clean in this season, similarly to other locations.[21] These are also the months in which high wind velocities are more frequent (Figure 2), also potentially contributing keeping the PV modules clean.[58] On the other hand, soiling builds up during the long dry summer until the first significant rain, typically occurring in between April and May.

Soiling losses are the results of the combination of cleaning events and deposition rates.[50] While rainfalls are the dominant cleaning events in most sites, deposition rates (i.e., soiling rates) can vary depending on a number of factors.[59] The analysis of the soiling rate distribution makes it possible to understand if this seasonal variability of soiling shown in Figure 6 is only the result of the natural cleanings' pattern or if it is also driven by other conditions. The bars in Figure 7 show the distribution of monthly mean soiling rates for all the investigated strings. These are obtained as weighted mean of all the soiling rates in a month, weighted according to the number of days they lasted.[50] The mean soiling rate varies from −0.03%/day in winter (July and August) to values <−0.10%/day in between January and May.

Differently from the results shown for other sites in Chile, and especially in Santiago, the investigated PV system experiences more severe soiling rates in summer than in winter. The difference can be related with the seasonal behavior of $PM_{2.5}$ and PM_{10}. These indexes quantify the mass of suspended particles of diameter <2.5 and <10 μm, respectively, in a cubic meter of air and have been found to be good predictors of soiling.[40,41] In Santiago, both the $PM_{2.5}$ and
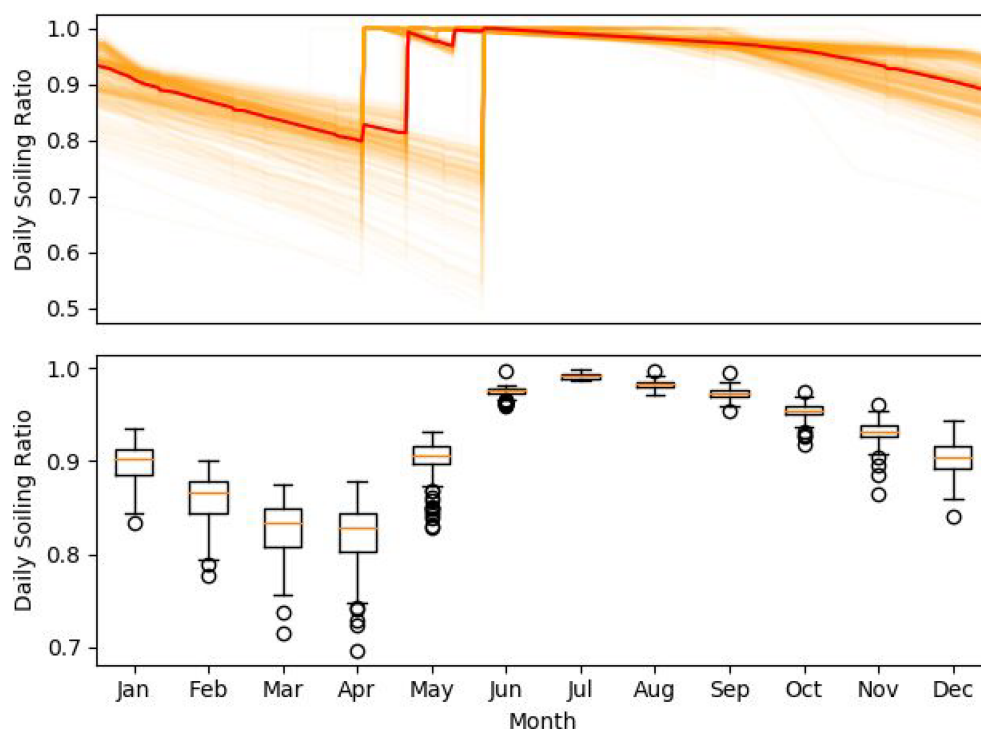
FIGURE 6 Three-year soiling profiles plotted over a 12-month period. Upper plot: soiling profiles. In red median of the soiling profiles. Lower plot: boxplots of the average daily soiling ratio in each month. The orange horizontal lines mark the medians, whereas the top and bottom limits of each box are the third and first quartile of the distribution (Q3 and Q1, respectively). The vertical lines in each boxplot are limited either by the lower or the upper whiskers (i.e., minimum and maximum values that are not outliers). The circles identify outliers, determined because outside of the Q1 − 1.5 * IQR to Q3 + 1.5 * IQR range, where IQR is calculated as Q3 − Q1
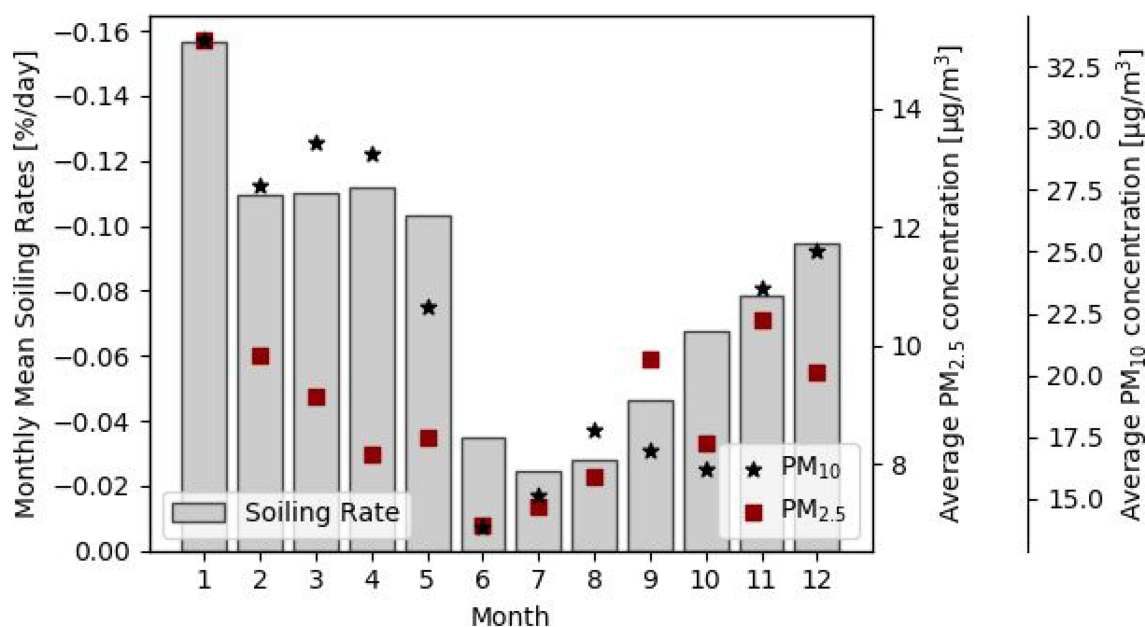
FIGURE 7 Monthly mean soiling rate distribution (left) and average daily $PM_{2.5}$ and PM_{10} concentrations (right). The monthly mean soiling rates are calculated using a referenced methodology proposed in a previous work[50] and considering only soiling rates <0%/day. The $PM_{2.5}$ data are calculated as mean of the 24-h averages downloaded from MERRA-2.[28] The PM_{10} data are calculated as mean of the daily averages downloaded from the SINCA database of the Chilean Ministry of the Environment[60]

PM_{10} peak in winter[5,20] because of the drop in wind speed experienced in the fall and winter seasons.[61] For the site investigated in this work, $PM_{2.5}$ was extracted[62] from MERRA-2 and PM_{10} from ground measurements, in both cases for the years 2017 to 2019. The $PM_{2.5}$ concentration, calculated using the equation reported in Provençal et al.,[63] reaches the minimum in between June and August (<8 μg/m^3)

and peaks from November to March (>9 μg/m^3), with a behavior similar to that found for the soiling rate. When the monthly average $PM_{2.5}$ values and the monthly mean soiling rates are compared, an R^2 of 0.52 is found (Figure S8). The daily PM_{10} concentrations, recorded by one monitor located 50 km east of the site,[60] confirm this trend, with minimum values in between June and October (<18 μg/m^3) and

maximum values in between January and April ($>27\ \mu g/m^3$). In this case, the correlation between PM_{10} and soiling rates has an R^2 of 0.88 (Figure S8). Therefore, the $PM_{2.5}$ and PM_{10} profiles justify the seasonal soiling rates trends at the investigated site and at the same time

explain the time difference compared to the losses previously reported for other locations.

Despite the high correlations between soiling rates and particle matter, it is worth noticing that the soiling extraction method used in
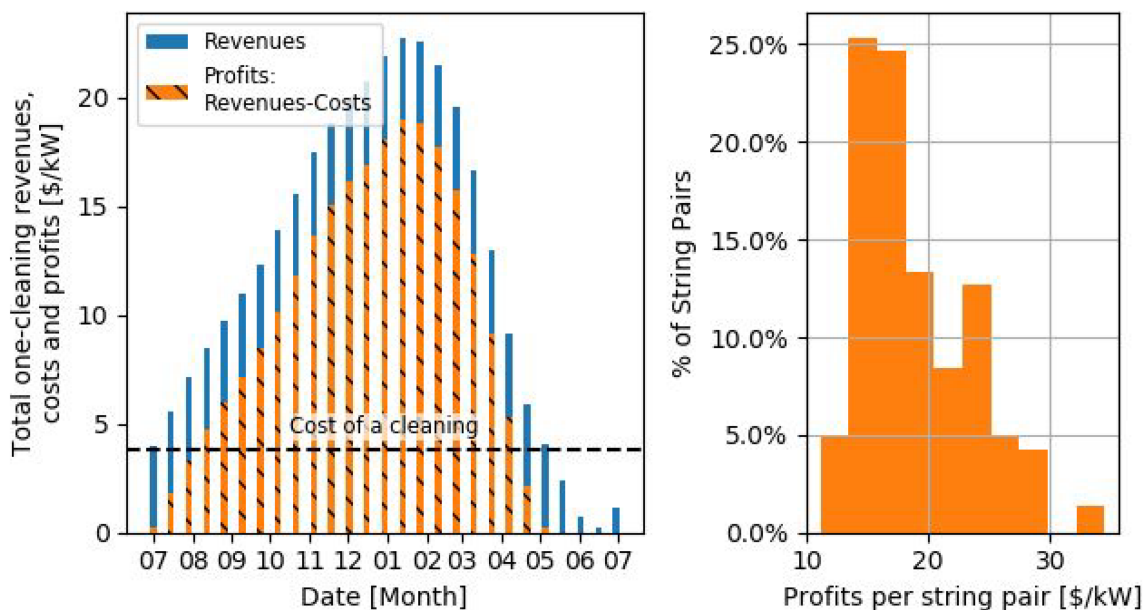
FIGURE 8 Left: revenues, costs, and profits in an optimal one-cleaning scenario depending on the cleaning date for the 2-year period in between July 2017 and June 2019. Right: histogram showing the profits made by each string pair on the most profitable cleaning date (January 13). The soiling and the energy profiles of the strings retuning the highest and the lowest profits are shown in Figure S9
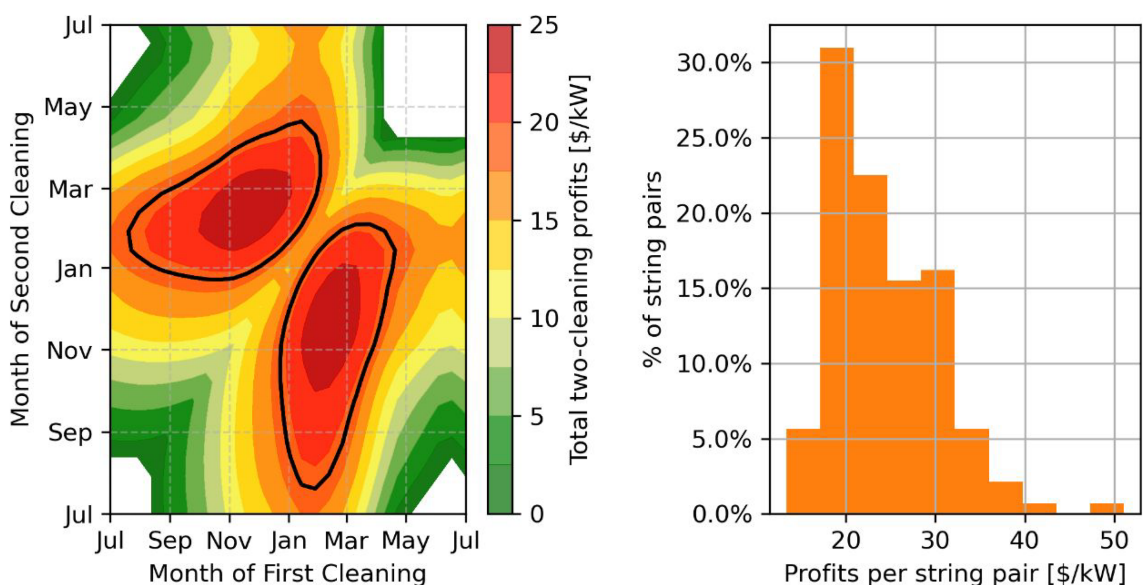
FIGURE 9 Left: profits due to a two-cleaning strategy, compared to a no-cleaning scenario, depending on the cleaning dates for the 2-year period in between July 2017 and June 2019. The cleaning costs are already subtracted from the profits. No color is shown if costs are larger than revenues. The black lines mark the maximum profits achievable through a single cleaning strategy (Figure 8). Right: histogram showing the profits made by each string pair on the optimal cleaning dates (November 18 and February 10). The soiling and the energy profiles of the strings retuning the highest and the lowest profits are shown in Figure S10

this work (Sections 3.3 and 3.4) differs from that used in previous analyses conducted in Chile.[5,20] The minimum number of 14 days and the R^2 requirements employed in this work lowered the number of soiling rates detected but were necessary to extract robust soiling loss profiles from the large number of strings. Similarly, the 0.03 threshold on cleaning reduced the number of cleanings and affected particularly minor cleaning events occurring in winter. In addition, previous works, conducted in different environments outside of Chile,[64–66] have highlighted that particle matter concentration is not necessarily the dominant factor controlling dust deposition. Further investigations should be therefore conducted in future to correlate the soiling rate values and a larger number of parameters.

5 | CLEANING COSTS AND PROFITS

5.1 | Cleaning frequency optimization

An analysis of the potential cleaning schedules is presented in this section. In order to get the most accurate results, cleaning optimization has to be performed on time series that start and end during the season with the least soiling losses. This way, the effect of each cleaning made on soiling intense periods can be prorogated until the following natural cleaning event and is not interrupted by the end of the time series. For the investigated location, as mentioned earlier, the most soiling intense period goes from October to May. For this reason, in this section, only the 2-year period going from July 1, 2017, to June 30, 2019, is considered, so that two complete soiling seasons (July to June) are analyzed. Limited soiling losses were recorded for all the valid strings (average ≤1%) on July 1 and June 30, the dates limiting this period.

In addition, in this section, the PV system is assumed to be made of the strings with valid soiling profiles only. Spatial interpolation has been used in the past to estimate the average soiling losses from nearby PV systems,[39] but no attempt has been made yet to model the daily soiling profile using spatial interpolation. The PV capacity of the valid strings sums up to 1.8 MW, which means that each cleaning costs >$3400.

By taking into account the soiling and the power output of all the valid strings, it is found that the most profitable day to clean, if only a cleaning per year is performed, falls in the week of January 13 (Figure 8). Cleaning is not profitable (revenues < cleaning costs) from mid-April to July. It should be noted that, because of the uneven soiling distribution shown in Figure 8, not all the strings return the same profits from the cleaning (right plot of Figure 8), with a factor up to 3× between most and less profitable strings (Figure S9).

If a two-cleaning scenario is chosen instead, the highest profits are found if the first cleaning is conducted in November and the second in February (left of Figure 9). In general, the soiling mitigation is the most profitable if at least one cleaning is conducted in between September and May, with the best results between January and March. A yearly two-cleaning strategy is more profitable than a one-cleaning approach if at least one of the cleanings is made in this 3-month period and the second one in between August and December. As also seen in Figure 9, cleanings return the minimum profits (if any) when at least one of them is conducted in between May and July.

The best results for a two-cleaning approach are found if the modules are cleaned on the weeks of November 18 and of February 10. This would increase the profits of soiling mitigation by 28% compared to a single cleaning approach. Similar to the one-cleaning scenario, not all the strings return the same profits when compared to a no-cleaning scenario (right of Figure 9).

Soiling mitigation profits are even higher if three cleanings are conducted per year (Figure 10). The best cleaning dates for a three-cleaning scenario fall in the weeks of November 4, January 13, and March 10 and return a maximum profit of $25.5/kW over the 2-year period. This is 34% higher than a single cleaning scenario. The soiling and the energy profiles of the strings returning the highest and the lowest profits for a three-cleaning scenario are shown in Figure S11. The soiling mitigation profits start to lower if more than three cleanings are performed. The drop in profits is limited to 4% to 5% if two or four cleanings are done; otherwise, it is more significant (profits reduced by >10% compared to optimal schedule). In all the modeled cleaning frequency scenarios (up to five cleanings per year), profits are higher if cleanings are done, compared to a scenario in
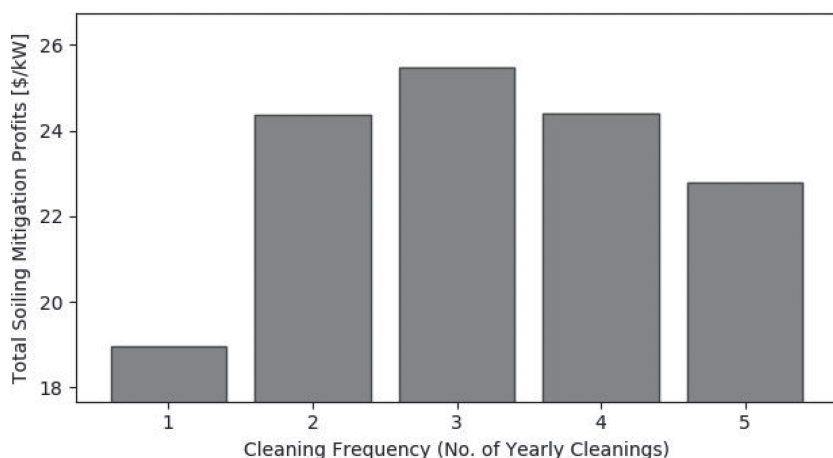
FIGURE 10 Total profits per cleaning strategy over the investigated 2-year period. The soiling and the energy profiles of the strings retuning the highest and the lowest profits for a three-cleaning scenario are shown in Figure S11

which no soiling mitigation is put in place. In addition, in all cases, the optimal artificial cleaning dates are in between September and March, the period in which most of the losses typically occur (Figure 4). The three cleanings per year conducted by the local O&M team were found to generate $24.3/MW, about 4% below the maximum achievable with an optimal three-cleaning schedule and in line with the profits returned by the best two-cleaning schedule.

It should be noted that the difference between the profits of an optimal three-cleaning strategy and those of optimal two- or four-cleaning strategies are minimal. Because of this, and because of the limited number of years available, it is not possible to draw any recommendation for the future years. Indeed, soiling can vary from year to year depending on (i) the interannual variability of the parameters influencing its rates of deposition and removal and (ii) the occurrence and the frequency of exceptional events, such as dust storms.[67] A larger number of years are generally needed to evaluate the seasonality of rainfalls and other weather variable responsible for soiling,[50] and more studies should be conducted, in future, on the advanced prediction of the optimal cleaning schedule.[68]

5.2 | String-optimized cleaning

As shown in Figures 8 and 9, given the same number of cleanings, not all the string pairs return the same profits, with factors of 3× between the highest and the lowest profit of each string. The same occurs for a frequency of three cleanings per year. This means that the site-wise most profitable cleaning frequency is not necessarily the most profitable for each individual string. The profits of each string in the various cleaning frequency scenarios can be mapped, as shown in Figure 11 for a three-cleaning approach, using the same methodology employed in Figure 5.

The soiling mitigation profit distribution shown in Figure 11 suggests that ideally it can be more profitable to clean only selected strings rather than the full PV system. At the given conditions, though, despite the soiling nonuniformity, it is found that only a limited number of the string pairs (4% of the total) would be more profitable in a two-cleaning rather than in a three-cleaning scenario. Because of this, a string-optimized cleaning schedule would improve the profits of soiling mitigation by less than 1% only. Despite that, this approach might become more beneficial in future as utility-scale PV systems get larger and therefore the effect of soiling nonuniformity is more pronounced. Indeed, the emissions of soiling sources located nearby a PV plants will more likely affect only few rows or strings of a large PV system rather than a whole PV plant. In smaller PV systems indeed, soiling is required to travel shorter distances to cover the entire PV surface and the wind patterns (and therefore the dust transportation) can be expected to be less impacted by the modules.

At the present stage, the results found for the investigated are difficult to generalize, as the soiling mechanisms will change with the PV system design, the tracking design, the distribution of soiling sources, and the wind pattern. So the costs and revenues of a string-
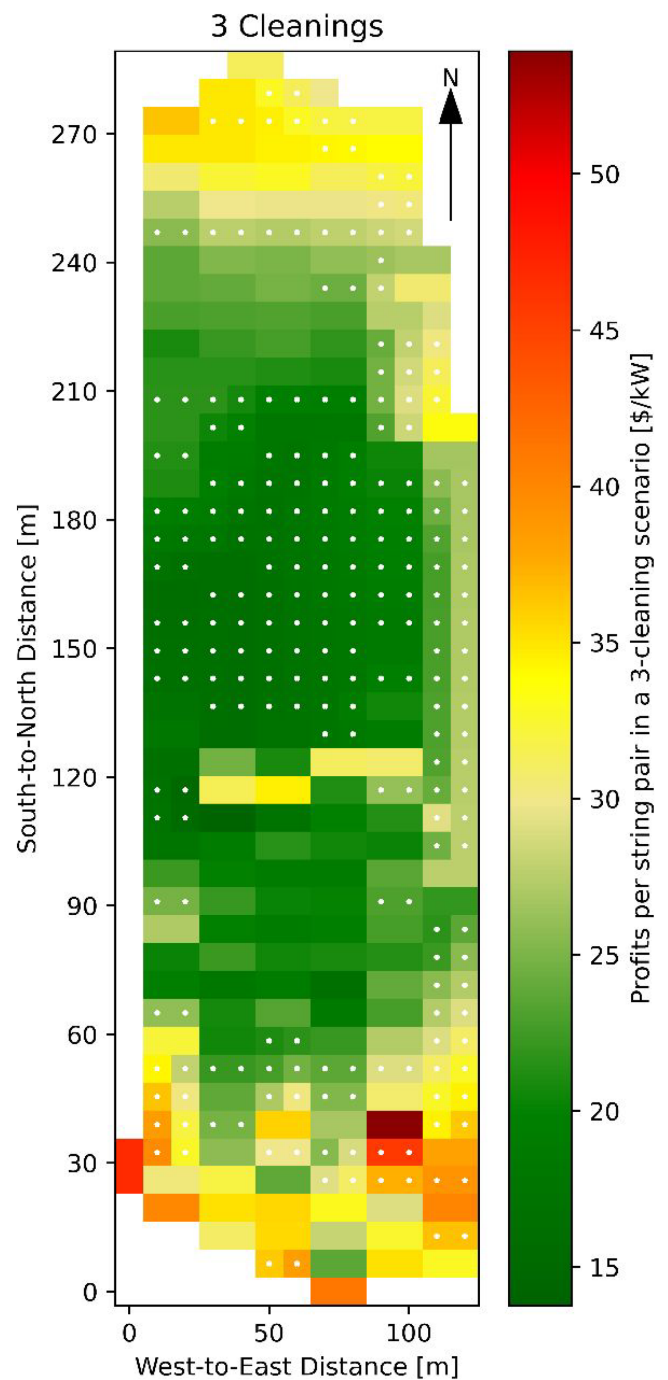
FIGURE 11 String pair specific soiling mitigation profits in a three-cleaning scenario. Each marker represents a string of 20 modules and is color coded depending on the magnitude of the profits (dark red: $53.9/kW, dark green: $13.8/kW). The profits of strings with nonvalid soiling profiles were estimated using linear spatial interpolation method available in the Python's SciPy package.[57] These strings are marked with a white dot

optimized cleaning should be estimated for each site as they depend on the location, on the severity of soiling, and on its distribution. In addition, it should be noted that the economic impact of nonuniform soiling and mitigation would change depending also on the economic

conditions, such as electricity price and cleaning costs, which are indeed discussed in the next section.

5.3 | Effect of cleaning cost and electricity Price

So far, a cost of $1.9/kW per cleaning was set. This is the minimum price offered by the different cleaning providers contacted by the authors of the report on the costs of PV cleaning in Chile.[55] In that work, the range of cleaning prices found for 100-kW rooftop PV systems was $1.9 to $87.1/kW. In addition, previous works took into account cleaning costs ranging from $1 to $13/kW.[5,20] So, given the variety of values used in previous references and considering that the cleaning cost of utility-scale systems can differ from that of rooftop systems, the analysis presented earlier was repeated. In this case, the cost of cleaning was varied from $1 to $90/kW, considering yearly zero- to three-cleaning scenarios.

The results of the analysis are shown in Figure 12. As expected, the optimal number of cleanings and the total soiling mitigation profits decreases as the cleaning cost raises. In particular, at the given conditions, soiling mitigation is no longer profitable if cleaning costs are ≥$12/kW. In addition, multiple yearly cleanings are less profitable

than a single cleaning when the costs are >$5/kW and become uneconomical when costs are >$8/kW per cleaning.

On the other hand, if the revenues and costs of soiling mitigation on the different string pairs are analyzed in each cleaning frequency scenario (right plot of Figure 12), it is found that soiling mitigation is no longer economically viable for most of strings for cleaning costs ≥$12/kW. However, soiling mitigation is still profitable for some strings for cleaning costs up to $18/kW. On the other hand, at least three cleanings per year are recommended for all the strings if cleanings cost ≤$1/kW.

At the given site, string specific cleanings do not become significantly profitable (raise in profits ≥1%) until the cleaning costs have raised up to $6/kW. Cleaning only economically worth strings can raise the soiling mitigation profits by as much as 18% for a cost of $10/kW. These values are within the $5 to $13/kW cleaning cost range considered in Cordero et al.,[20] but above the $1 to $4/kW range considered by other studies,[5,22] all conducted in Chile in between 2017 and 2018. Above $10/kW, cleaning some strings is the only economically worth approach, as cleaning the full PV site costs more than the revenues made with the recovered energy.

In addition to the cleaning costs, it should be considered that additional parameters can affect the profitability of soiling
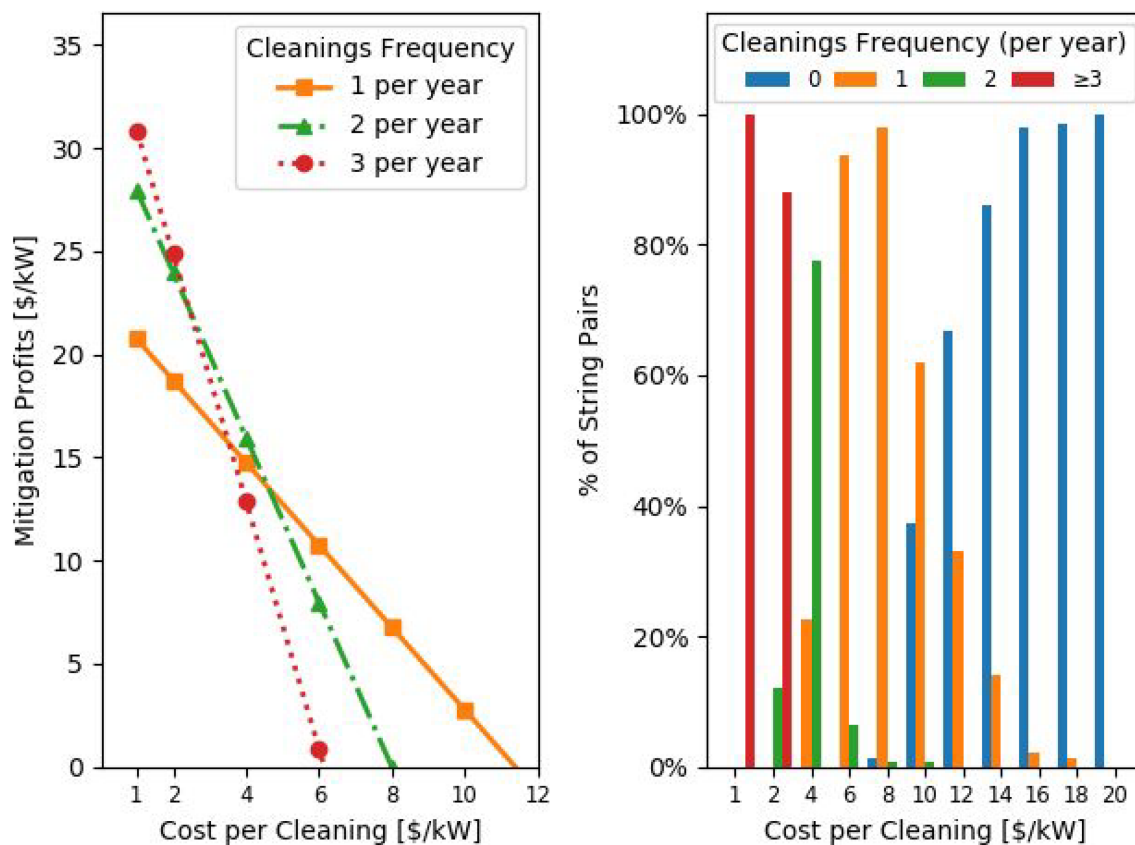
FIGURE 12 Left: soiling mitigation profits for different cleaning frequencies and different cleaning costs. Only combinations that lead to profits >0 are shown. Right: number of strings in which each cleaning frequency is the most profitable depending on the cost per cleaning. Analysis conducted by varying the cleaning costs of $1 and $2/kW and multiples up to a maximum of $90/kW. A maximum of three cleanings per year has been modeled

FIGURE 13 Soiling mitigation profits for various cleaning frequencies, electricity prices, and cleaning costs. Each line represents a different cleaning cost scenario. The number of yearly cleanings recommended for each combination of electricity price and cleaning cost (i.e., the cleaning frequency returning the maximum profits) can be identified through the shape of the markers. A maximum of three cleanings per year has been modeled
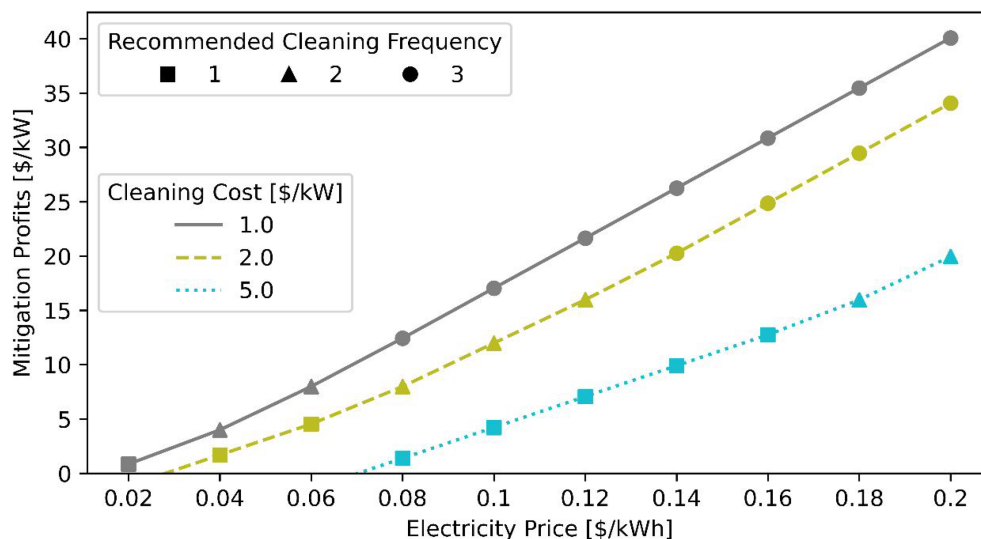
mitigation.[38,49] One of these is the electricity price: Higher prices favor soiling mitigation as they increase the revenues made per cleaning. Therefore, the cleaning frequency has to be adjusted according also to the electricity price, whose values can even vary with time. So a sensitivity analysis is here repeated taking into account electricity prices ranging from $0.20/kWh to as low as $0.02/kWh (Figure 13). As expected, the profits in soiling mitigation and the number of recommended cleanings increase with the electricity price. At the cleaning costs of $1.9/kW, no more than one cleaning per year is recommended for electricity prices ≤€0.06/kWh, and mitigation becomes unprofitable for electricity prices <€0.04/kWh. However, these results also change depending on the cleaning costs: Lower cleaning costs would make more frequent cleanings potentially more profitable, even for lower electricity prices (and vice versa).

6 | CONCLUSIONS

In the present study, the soiling losses occurred on a 3.25-MW PV system deployed in Chile have been investigated through the implementation of a robust soiling extraction methodology. The study covers a 3-year period from 2017 to the end of 2019 and considers 142 DC power time series measured from the 508 strings of the PV plant.

The paper investigates the effect of nonuniform soiling loss distribution. While all the strings are subject to the same qualitative soiling trends, with summer being the most soiling intense period due to infrequent rainfalls and severe soiling deposition rates, significant differences in the absolute values of the soiling losses are found among the strings of the sites. In particular, the highest soiling losses are experienced by the strings closest to the main trafficked road and to an unpaved area where heavy vehicles operate. Losses are found to be twice as high in these strings than in those at the center of the plant. The nonuniformity is mainly driven by different soiling

deposition rates, with a median factor of 2× to 3× between the highest and the lowest soiling rates occurring in summer.

The investigation also shows the optimal mitigation strategies for various electricity prices and cleaning costs, with three recommended cleanings per year at a cleaning cost of $1.9/kW and at an electricity price of $0.16/kWh. A drop in profits of ∼4% is estimated if two or four cleanings per year are done compared to the optimal schedule. In all cases, the uneven distribution of soiling is also found to affect the cleaning optimization, as ratios of 3× are found between the maximum and the minimum profits made by cleaning at the same time the most and least soiled strings of the PV system. For this reason, the possibility of cleaning only economically worth strings instead of the full PV system is discussed.

Soiling nonuniformity is expected to become more important with the increase in size of the PV systems, as the effects of soiling point sources might become more localized and selected strings cleanings might become more feasible. This work represents a first step toward the understanding of this phenomenon. Additional data from more sites will have to be analyzed and shared to make it possible to develop a broadly applicable model. The results indicate that more studies should be conducted on the causes, the economics, and the mitigation of nonuniform soiling. In addition to the energy profiles, also locally measured environmental parameters should be analyzed to improve the understanding and the modeling of this phenomenon.

Furthermore, the present work discusses the challenges encountered in the extraction of soiling from a large number of PV performance time series, even if measured within the same site. Making use of PV plant data rather than soiling sensor's data widens the number of data sources potentially available but, at the same time, increases the complexity of the analysis. For this reason, future works should address some of the questions that are still open in soiling modeling and that were raised in this work (i.e., the identification of natural cleanings, the potential soiling of the irradiance sensors, and the nonlinearity of the soiling rates).

DATA AVAILABILITY STATEMENT

Research data are not shared.

ORCID

Leonardo Micheli https://orcid.org/0000-0001-7986-7560
Eduardo F. Fernández https://orcid.org/0000-0001-7934-9755
Álvaro Fernández-Solas https://orcid.org/0000-0003-4650-9470
João Gabriel Bessa https://orcid.org/0000-0002-2095-2282
Florencia Almonacid https://orcid.org/0000-0001-7352-2377

REFERENCES

1. Ilse K, Micheli L, Figgis BW, et al. Techno-economic assessment of soiling losses and mitigation strategies for solar power generation. *Joule*. 2019;3(10):2303-2321. https://doi.org/10.1016/j.joule.2019.08.019

2. Costa SCS, Diniz ASAC, Kazmerski LL. Dust and soiling issues and impacts relating to solar energy systems: Literature review update for 2012–2015. *Renew Sustain Energy Rev*. 2016;63:33-61. https://doi.org/10.1016/j.rser.2016.04.059

3. Costa SCS, Diniz ASA, Kazmerski LL. Solar energy dust and soiling R&D progress: literature review update for 2016. *Renew Sustain Energy Rev*. 2018;82:2504-2536.

4. You S, Lim YJ, Dai Y, Wang C-H. On the temporal modelling of solar photovoltaic soiling: Energy and economic impacts in seven cities. *Appl Energy*. 2018;228:1136-1146. https://doi.org/10.1016/j.apenergy.2018.07.020

5. Besson P, Munoz C, Ramirez-Sagner G, Salgado M, Escobar R, Platzer W. Long-term soiling analysis for three photovoltaic technologies in Santiago region. *IEEE J Photovolt*. 2017;7(6):1755-1760. https://doi.org/10.1109/jphotov.2017.2751752

6. Rodrigo PM, Gutiérrez S, Micheli L, Fernández EF, Almonacid FM. Optimum cleaning schedule of photovoltaic systems based on levelised cost of energy and case study in central Mexico. *Sol Energy*. 2020;209:11-20. https://doi.org/10.1016/j.solener.2020.08.074

7. Jones RK, Baras A, Saeeri AA, et al. Optimized cleaning cost and schedule based on observed soiling conditions for photovoltaic plants in central Saudi Arabia. *IEEE J Photovolt*. 2016;6(3):730-738. https://doi.org/10.1109/jphotov.2016.2535308

8. Gostein M, Passow K, Deceglie MG, Micheli L, Stueve B. Local variability in PV soiling rate. *35th European Photovoltaic Solar Energy Conference and Exhibition. Bruxelles, Belgium*. 2018;1979-1983.

9. Gostein M, Passow K, Deceglie MG, Micheli L, Stueve B. Local variability in PV soiling rate. In: IEEE 7th World Conference on Photovoltaic Energy Conversion (WCPEC-7). Waikoloa, HI; 2018. 3421-3425.

10. Etyemezian V, Nikolich G, Gillies JA. Mean flow through utility scale solar facilities and preliminary insights on dust impacts. *J Wind Eng Ind Aerodyn*. 2017;162:45-56. https://doi.org/10.1016/j.jweia.2017.01.001

11. Gostein M, Caron JR, Littmann B. Measuring soiling losses at utility-scale PV power plants. *2014 IEEE 40th Photovolt Spec Conf*. 2014;885–890. Available from: http://ieeexplore.ieee.org/lpdocs/epic03/wrapper.htm?arnumber=6925056

12. International Electrotechnical Commission. Photovoltaic system performance—part 1: monitoring (IEC 61724-1, Edition 1.0, 2017-03). Geneva, Switzerland: IEC; 2017.

13. Olson D, Bakken BE. Utility-scale solar PV: from big to biggest [Internet]. DVN GI 2019. Available from: https://www.dnvgl.com/feature/utility-scale-solar.html

14. Comisión Nacional de Energía. Reporte Mensual Energia Renovable No Concencional (ERNC) - Septiembre 2020 (Vol. No. 49) [Internet]. Santiago, Chile; 2020. Available from: https://www.cne.cl/wp-content/uploads/2020/09/RMensual_ERNC_v202009.pdf

15. Comisión Nacional de Energía. Reporte Sector Energetico— Septiembre 2020 (Vol. No. 67) [Internet]. Santiago, Chile; 2020. Available from: https://www.cne.cl/wp-content/uploads/2020/09/RMensual_v202009.pdf

16. REN21. Renewables 2020 Global Status Report. Paris; 2020.

17. Zurita A, Castillejo-Cuberos A, García M, et al. State of the art and future prospects for solar PV development in Chile. *Renew Sustain Energy Rev*. 2018;92:701-727. https://doi.org/10.1016/j.rser.2018.04.096

18. Bloomberg New Energy Finance. Chile Power System Outlook. 2019; (December). Available from: https://data.bloomberglp.com/professional/sites/24/Flexibility-Solutions-for-High-Renewable-Energy-Systems-Chile-Outlook.pdf

19. IEA PVPS. Trends in photovoltaic applications 2019 [Internet]. 2020. Available from: https://iea-pvps.org/wp-content/uploads/2020/02/5319-iea-pvps-report-2019-08-lr.pdf

20. Cordero RR, Damiani A, Laroze D, et al. Effects of soiling on photovoltaic (PV) modules in the Atacama Desert. *Sci Rep*. 2018;8(1):1-14.

21. Urrejola E, Antonanzas J, Ayala P, et al. Effect of soiling and sunlight exposure on the performance ratio of photovoltaic technologies in Santiago, Chile. *Energy Convers Manag*. 2016;114:338-347. https://doi.org/10.1016/j.enconman.2016.02.016

22. Luque EG, Antonanzas-Torres F, Escobar R. Effect of soiling in bifacial PV modules and cleaning schedule optimization. *Energy Convers Manag*. 2018;174:615-625. https://doi.org/10.1016/j.enconman.2018.08.065

23. Olivares D, Ferrada P, de Matos C, et al. Characterization of soiling on PV modules in the Atacama Desert. *Energy Procedia*. 2017;124:547-553. https://doi.org/10.1016/j.egypro.2017.09.263

24. Ferrada P, Araya F, Marzo A, Fuentealba E. Performance analysis of photovoltaic systems of two different technologies in a coastal desert climate zone of Chile. *Sol Energy*. 2015;114:356-363. https://doi.org/10.1016/j.solener.2015.02.009

25. Olivares D, Ferrada P, Bijman J, et al. Determination of the soiling impact on photovoltaic modules at the coastal area of the Atacama Desert. *Energies*. 2020;13(15):3819.

26. Kottek M, Grieser J, Beck C, Rudolf B, Rubel F. World map of the Köppen-Geiger climate classification updated. *Meteorol Zeitschrift*. 2006;15(3):259-263. https://doi.org/10.1127/0941-2948/2006/0130

27. World Bank Group (US). Global solar atlas [Internet]. Available from: https://globalsolaratlas.info

28. Global Modeling and Assimilation Office (GMAO). MERRA-2 tavg1_2d_slv_Nx: 2d, 1-hourly, time-averaged, single-level, assimilation, single-level diagnostics V5.12.4. Greenbelt, MD, USA; 2019.

29. International Electrotechnical Commission. IEC 61724-1— photovoltaic system performance monitoring—guidelines for measurement, data exchange, and analysis (Part 1). Geneva, Switzerland: IEC; 2017.

30. soda-pro [Internet]. Available from: http://www.soda-pro.com/

31. Holmgren WF, Hansen CW, Mikofski MA. pvlib python: A python package for modeling solar energy systems. *J Open Source Softw.* 2018;3(29):884. https://doi.org/10.21105/joss.00884

32. King DL, Boyson WE, Kratochvill JA. Photovoltaic array performance model [Internet]. Albuquerque, New Mexico; 2004. Available from: http://prod.sandia.gov/techlib/access-control.cgi/2004/043535.pdf

33. Erbs DG, Beckman WA, Klein SA. Estimation of degree-days and ambient temperature bin data from monthly-average temperatures. *ASHRAE Journal.* 1983;25(6):60-65.

34. ASHRAE standard 93-77.

35. Kasten F, Young AT. Revised optical air mass tables and approximation formula. *Appl Opt.* 1989;28(22):4735-4738. Available from: http://ao.osa.org/abstract.cfm?URI=ao-28-22-4735

36. Gueymard C. Critical analysis and performance assessment of clear sky solar irradiance models using theoretical and measured data. *Sol Energy.* 1993;51(2):121-138. https://doi.org/10.1016/0038-092x(93)90074-x

37. Theristis M, Livera A, Jones CB, Makrides G, Georghiou GE, Stein JS. Nonlinear photovoltaic degradation rates: modeling and comparison against conventional methods. *IEEE J Photovolt.* 2020;10(4):1112-1118. https://doi.org/10.1109/jphotov.2020.2992432

38. Micheli L, Fernández EF, Aguilera JT, Almonacid F. Economics of seasonal photovoltaic soiling and cleaning optimization scenarios. *Energy.* 2021;215:119018. https://doi.org/10.1016/j.energy.2020.119018

39. Micheli L, Deceglie MG, Muller M. Mapping photovoltaic soiling using spatial interpolation techniques. *IEEE J Photovolt.* 2019;9(1):272-277. https://doi.org/10.1109/jphotov.2018.2872548

40. Micheli L, Deceglie MG, Muller M. Predicting photovoltaic soiling losses using environmental parameters: an update. *Prog Photovolt Res Appl.* 2019;27(3):210-219. https://doi.org/10.1002/pip.3079

41. Micheli L, Muller M. An investigation of the key parameters for predicting PV soiling losses. *Prog Photovolt Res Appl.* 2017;25(4):291-307. http://www.scopus.com/inward/record.url?eid=2-s2.0-85015881300%26partnerID=MN8TOARS

42. Micheli L, Theristis M, Livera A, et al. Improved PV soiling extraction through the detection of cleanings and change points. *IEEE J Photovolt.* 2021;11(2):519-526. https://doi.org/10.1109/jphotov.2020.3043104

43. Deceglie MG, Micheli L, Muller M. Quantifying soiling loss directly from PV yield. *IEEE J Photovolt.* 2018;8(2):547-551. https://doi.org/10.1109/jphotov.2017.2784682

44. NREL. RdTools, version (1.2.2). 2018.

45. Jordan DC, Deline C, Kurtz SR, Kimball GM, Anderson M. Robust PV degradation methodology and application. *IEEE J Photovolt.* 2018;8(2):525-531. https://doi.org/10.1109/jphotov.2017.2779779

46. Micheli L, Muller M, Fernandez EF, Fernández EF, Almonacid FM. Segmentation of deposition periods: an opportunity to improve PV soiling extraction. *IEEE 45th Photovoltaic Specialist Conference (PVSC).* 2020;595-598.

47. Deceglie MG, Muller M, Defreitas Z, Kurtz S. A scalable method for extracting soiling rates from PV production data. *2016 IEEE 43rd Photovoltaic Specialist Conference (PVSC).* 2016;2061-2065.

48. Kimber A, Mitchell L, Nogradi S, Wenger H. The effect of soiling on large grid-connected photovoltaic systems in California and the Southwest Region of the United States. In: *2006 IEEE 4th World Conference on Photovoltaic Energy Conference.* 2006. 2:2391–2395.

49. Micheli L, Theristis M, Talavera DL, Almonacid F, Stein JS, Fernández EF. Photovoltaic cleaning frequency optimization under different degradation rate patterns. *Renew Energy.* 2020;166:136-146. https://doi.org/10.1016/j.renene.2020.11.044

50. Micheli L, Fernandez EF, Muller M, Almonacid F. Extracting and generating PV soiling profiles for analysis, forecasting, and cleaning optimization. *IEEE J Photovolt.* 2020;10(1):197-205. https://doi.org/10.1109/jphotov.2019.2943706

51. Caron JR, Littmann B. Direct monitoring of energy lost due to soiling on first solar modules in California. *IEEE J Photovolt.* 2013;3(1):336-340. https://doi.org/10.1109/jphotov.2012.2216859

52. Toth S, Hannigan M, Vance M, Deceglie M. Predicting photovoltaic soiling from air quality measurements. *IEEE J Photovolt.* 2020;10(4):1142-1147. https://doi.org/10.1109/jphotov.2020.2983990

53. Gostein M, Duster T, Thuman C. Accurately measuring PV soiling losses with soiling station employing module power measurements. In: IEEE 42nd Photovoltaic Specialist Conference (PVSC). 2015;1–4.

54. Skomedal A, Haug H, Marstein ES. Endogenous soiling rate determination and detection of cleaning events in utility-scale PV plants. *IEEE J Photovolt.* 2019;9(3):858-863. https://doi.org/10.1109/jphotov.2019.2899741

55. Ministerio de Energía (MINENERGIA), Deutsche Gesellschaft für Internationale Zusammenarbeit (Sociedad Alemana de Cooperación Internacional - GIZ). Informe Ofertas Recibidas para la Consultoría "Ejecución de limpieza módulos de plantas fotovoltaicas (FV) construidas a través del Programa Techos Solares Públicos (PTSP) del Ministerio De Energía" 2016.

56. Jones E, Oliphant E, Peterson P, et al. SciPy: Open Source Scientific Tools for Python [Internet]. 2001. Available from: http://www.scipy.org/

57. Moghimi MA, Ahmadi G. Wind barriers optimization for minimizing collector mirror soiling in a parabolic trough collector plant. *Appl Energy.* 2018;225:413-423. https://doi.org/10.1016/j.apenergy.2018.05.027

58. Javed W, Guo B, Figgis B. Modeling of photovoltaic soiling loss as a function of environmental variables. *Sol Energy.* 2017;157:397-407. https://doi.org/10.1016/j.solener.2017.08.046

59. Figgis B, Ennaoui A, Ahzi S, Rémond Y. Review of PV soiling particle mechanics in desert environments. *Renew Sustain Energy Rev.* 2017;76:872-881. https://doi.org/10.1016/j.rser.2017.03.100

60. Ministerio del Medio Ambiente. Sistema de Información Nacional de Calidad del Aire (SINCA) [Internet]. [cited 2020 Sep 9]. Available from: https://sinca.mma.gob.cl/index.php/

61. Cordero RR, Seckmeyer G, Damiani A, et al. Aerosol effects on the UV irradiance in Santiago de Chile. *Atmos Res.* 2014;149:282-291. https://doi.org/10.1016/j.atmosres.2014.07.002

62. Global Modeling and Assimilation Office (GMAO). MERRA-2 tavg1_2d_aer_Nx: 2d, 1-hourly, time-averaged, single-level, assimilation, aerosol diagnostics 0.625 x 0.5 degree V5.12.4 (M2T1NXAER).

63. Provençal S, Buchard V, da Silva AM, Leduc R, Barrette N. Evaluation of PM surface concentrations simulated by Version 1 of NASA's MERRA Aerosol Reanalysis over Europe. *Atmos Pollut Res.* 2017 Mar; 8(2):374-382. https://doi.org/10.1016/j.apr.2016.10.009

64. Figgis B, Guo B, Javed W, Ahzi S, Rémond Y. Dominant environmental parameters for dust deposition and resuspension in desert climates. *Aerosol Sci Technol.* 2018;52(7):788-798. https://doi.org/10.1080/02786826.2018.1462473

65. Valerino M, Bergin M, Ghoroi C, Ratnaparkhi A, Smestad GP. Low-cost solar PV soiling sensor validation and size resolved soiling impacts: A comprehensive field study in Western India. *Sol Energy.* 2020;204:307-315. https://doi.org/10.1016/j.solener.2020.03.118

66. Isaifan RJ, Johnson D, Ackermann L, Figgis B, Ayoub M. Evaluation of the adhesion forces between dust particles and photovoltaic module surfaces. *Sol Energy Mater Sol Cells.* 2019;191:413-421. https://doi.org/10.1016/j.solmat.2018.11.031

67. Deceglie MG, Micheli L, Muller M Quantifying year-to-year variations in solar panel soiling from PV energy-production data. In: 2017 IEEE 44th Photovoltaic Specialist Conference (PVSC). Washington, D.C., IEEE; 2017:2804–2807.

68. Micheli L, Fernández EF, Almonacid F. Photovoltaic cleaning optimization through the analysis of historical time series of environmental parameters. *Sol Energy*. 2021;227:645-654. https://doi.org/10.1016/j.solener.2021.08.081

SUPPORTING INFORMATION

Additional supporting information may be found in the online version of the article at the publisher's website.